Molecular Channel Fading due to Diffusivity Fluctuations

Song Qiu[1], Taufiq Asyhari[2], Weisi Guo[1*] Siyi Wang[3], Bin Li[4], Chenglin Zhao[4], Mark Leeson[1]

***Abstract*—Molecular Communications via Diffusion (MCvD) is sensitive to environmental changes such as the diffusion coefficient (mass diffusivity). The diffusivity is directly related to a number of parameters including the ambient temperature, which varies slowly over time. Whilst molecular noise models have received significant attention, channel fading has not been extensively considered. Using experimental data, we show that the ambient temperature varies approximately according to a Normal distribution. As a result, we analytically derive the fading distribution and validate it using numerical simulations. We further derive the joint distribution of the channel gain and the additive noise, and examine the impact of such interactions on the ISI distribution, which is shown to conform to a Generalised Extreme Value (GEV) distribution.**

I. Introduction

Over the past few decades, human society has achieved reliable wireless communications using predominantly electromagnetic (EM) waves. However, we understand very little about how to communicate at the micro- and nano-scales ($<$m^{-5}). In the past few years, there has been a growing research in molecular communications for application areas such as targeted drug delivery [1]. In such environments, traditional notions of radio-wave antenna design and propagation falter due to the small antenna size and transmit energy restrictions, as well as the complex propagation channels involved. Inspired by biological communications, conveying data using chemical molecules has served as an inspiration for communication engineers, leading to an increasing understanding of channel models and appropriate physical layer designs [2].

Channel models are important in deriving the effective channel capacity, designing effective coding and advancing signal processing algorithms. Consider the transmitter emitting x molecules, which undergo diffusion. The receiver at a distance d away samples at a certain time instance t, receives y molecules, such that $y = \phi x + n$, where the channel gain is $\phi(d, t)$, the transmitted signal is x, and the additive noise is n. In a realistic Molecular Communications via Diffusion (MCvD) system, additive noise can arise for many reasons and it is difficult to take all of them into account or argue which may dominate. One form of noise is known as *counting noise*, which arises from the random arrival of molecules [3], [4].

To the best of our knowledge, existing research [5] has assumed that the value of ϕ is constant for a fixed time and distance, and variations in the diffusion channel due to random environment changes have been neglected (i.e., channel fading has not been considered in a molecular communication context). Despite the abundance of additive noise based research [3], [4], [6], an examination of how variations in the channel gain itself affect performance has been lacking. Most existing papers assume a synchronized system, whereby each pulse is sampled at its peak response [4]. One recent paper has examined how long term temperature changes affect the MCvD channel performance [7], but did not consider how continuous temporal variations affect bit level performance (e.g., biological systems with short distance communications ($\sim \mu$m - $\sim$mm) suffer from temporal variations due to internal *kinetic energy* transfer or external temperature shift [8]). Whilst it is well established that the mass diffusivity (diffusion coefficient) can vary due to three parameters: (1) the temperature of the medium, (2) the radius of the molecule, and (3) the dynamic viscosity, the resulting impact on communication performance due to continuous and random changes has been neglected.

The main contribution of this paper is to show the following: (1) temperature variations in an environment are approximately Normally distributed, which leads to a Normally-distributed diffusivity, (2) consequentially, the channel gain has closed-form expressions of cumulative distribution function (CDF) and probability density function (PDF), (3) the joint distribution of channel gain and the additive noise, and (4) the impact on the inter-symbol interference (ISI) distribution.

II. Channel Gain

A. Theoretical Analysis

Let us consider the diffusion channel gain ϕ, which can be found via averaging the motion of random walk particles [9] or solving the partial differential equation (PDE) in Fick's Law. We assume that the transmitter utilizes on-off-keying (OOK) to encode and transmit data across 1-dimensional pipe networks (semi-infinite space) [10] and the receiver is passive (i.e., optical molecular counter) such that

$$\phi\left(d,t\right) = \frac{e^{-\frac{d^2}{4Dt}}}{\sqrt{\pi D t}} \tag{1}$$

where D is the diffusivity. It is worth noting that the following analysis can be performed more generally for either higher dimensions or molecule capture scenarios (i.e., first passage distribution [11]) or both. The time delay to peak pulse $t_{\max}$ can be found from $\frac{\mathrm{d}\phi}{\mathrm{d}t} = 0$ to be:

$$t_{\max} = \frac{d^2}{2D}, \quad \text{and} \quad D = \frac{d^2}{2t_{\max}}. \tag{2}$$

[1]Song Qiu, Weisi Guo ([*]corresponding author: Weisi.Guo@warwick.ac.uk), and Mark Leeson are with the University of Warwick, UK. [2]Taufiq Asyhari is with University of Bradford, UK. [3]Siyi Wang is with Xi'an Jiaotong Liverpool University, China. [4]Bin Li and Chenglin Zhao are with Beijing University of Posts and Telecommunications, China. This research is supported by US Air Force grant 16IOE064, and Royal Society & NSFC co-fund grant IE150708.

By inserting the value of $t = t_{\max}$ in (2) into (1), we can find the peak received gain value $\phi_{\max}$. Plotting ϕ versus t (for a fixed D) and plotting ϕ versus D (for a given t) will produce a similar trend. Therefore, when t is fixed to $t = t_{\max}$, the relationship of ϕ against D has a similar behavior to that of Fig. 1. From here we can identify that variation of D due to temperature fluctuation will lead to ϕ being randomly distributed over a finite support of $[0, \phi_{\max}]$.

As shown by the experimental data in the Appendix, the room temperature T follows a Normal (i.e., Gaussian) distribution $T \sim \mathcal{N}(\mu, \sigma^2)$. The Normal distribution found empirically in the lab can also be used to model human body temperature variations [12]. In vivo environments, the Reynolds number is typically close to zero [1], and hence we can apply the *Stokes-Einstein* equation [13]:

$$D = kT, \quad \text{where: } k = \frac{k_B}{6\pi\eta R_H} \tag{3}$$

where k_B is Boltzmann's constant, η is the dynamic viscosity of the medium, and R_H is the stoke's radius of the spherical molecules carrying information. Equation (3) implies that D follows a Normal distribution as $D \sim \mathcal{N}(k\mu, k^2\sigma^2)$, where $\overline{D} = k\mu$ and $k^2\sigma^2$ denote the mean and variance of the diffusivity value.

We assume the receiver has the knowledge of the environment average temperature and it can determine the sample time $t_{\max}$, which is fixed based on the average value of D, such that $\bar{t}_{\max} = d^2/2\overline{D}$. We assume the receiver samples at this fixed time interval and observes fluctuations to the peak response value of $\phi_{\max}$. As illustrated in Fig. 1, any variations in the diffusivity will cause the peak of the pulses to arrive earlier or later than expected. Given a fixed sampling time of $\bar{t}_{\max}$, the resulting received signal value will fluctuate and always be smaller than $\phi_{\max}$. As shown in Fig. 1, the original peak value of $\phi_{\max}$ (labelled 1.) will degrade as a result of either the channel's higher temperature (labelled 2.) or lower temperatures (labelled 3.). Note that we cannot simply see how the peak response $\phi_{\max}$ varies as a function of diffusivity D, as the sample time $\bar{t}_{\max}$ will no longer be aligned with the peak response of the shifted pulses. We also assume the temperature varies consistently across the channel, provided the transmission distance is not too long.

In order to find out the distribution of the generic channel gain Φ, we first express D in terms of ϕ according to (1), i.e.,

$$D(\phi) = -\frac{d^2}{2tW\left[-\frac{(\phi d)^2\pi}{2}\right]}, \tag{4}$$

where $W(\cdot)$ is the product log function (*Lambert W* Function). Note that ϕ is not a monotonously increasing function of D, thus a standard inverse mapping to find the density of function of ϕ cannot be directly applied. In fact, for a given value of ϕ (except for $\phi_{\max}$), there exist two values of D, namely $D = \ell_-$ and $D = \ell_+$, that satisfy (1), i.e.,

[1]Reynolds number is a dimensionless number used in fluid mechanics to indicate whether fluid flow past a body or in a duct is steady or turbulent. When the Reynolds number is close to 0, then the mass velocity in the environment is close to 0.

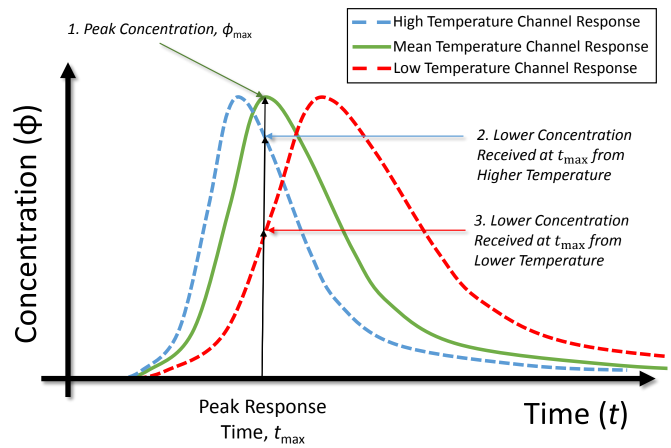

Fig. 1. Illustration of temperature variations on the peak concentration received at the receiver.

$$\ell_- = -\frac{d^2}{2tW_{-1}\left[-\frac{(\phi d)^2\pi}{2}\right]}, \quad \ell_+ = -\frac{d^2}{2tW_0\left[-\frac{(\phi d)^2\pi}{2}\right]}, \tag{5}$$

such that $\ell_- < \ell_+$, where $W_{-1}[\cdot]$ and $W_0[\cdot]$ are the lower and upper branches of the Lambert W function. The CDF can then be evaluated as follows.

$$\begin{aligned} F_\Phi(\phi) &= \Pr\{\Phi < \phi\} \\ &= \Pr\{D < \ell_-\} + \Pr\{D > \ell_+\} \\ &= \frac{1}{2}\left(1 + \operatorname{erf}\left[\frac{\ell_- - k\mu}{k\sigma\sqrt{2}}\right]\right) + \frac{1}{2}\left(1 - \operatorname{erf}\left[\frac{\ell_+ - k\mu}{k\sigma\sqrt{2}}\right]\right) \\ &= 1 + \frac{1}{2}\operatorname{erf}\left[\frac{1}{k\sigma\sqrt{2}}\left(-\frac{d^2}{2tW_{-1}\left[-\frac{(\phi d)^2\pi}{2}\right]} - k\mu\right)\right] \\ &\quad - \frac{1}{2}\operatorname{erf}\left[\frac{1}{k\sigma\sqrt{2}}\left(-\frac{d^2}{2tW_0\left[-\frac{(\phi d)^2\pi}{2}\right]} - k\mu\right)\right], \end{aligned} \tag{6}$$

where $\operatorname{erf}(\cdot)$ is the Gaussian error function. The PDF $f_\Phi(\phi)$ can then be obtained by

$$\begin{aligned} f_\Phi(\phi) = \frac{\partial F_\Phi(\phi)}{\partial \phi} &= \frac{1}{k\sigma\sqrt{2\pi}} e^{-\frac{(\ell_- - k\mu)^2}{2k^2\sigma^2}} \cdot \frac{\partial \ell_-}{\partial \phi} \\ &\quad - \frac{1}{k\sigma\sqrt{2\pi}} e^{-\frac{(\ell_+ - k\mu)^2}{2k^2\sigma^2}} \cdot \frac{\partial \ell_+}{\partial \phi} \end{aligned} \tag{7}$$

where

$$\frac{\partial \ell_-}{\partial \phi} = \frac{d^2}{\phi t W_{-1}\left[-\frac{(\phi d)^2\pi}{2}\right]\left(1 + W_{-1}\left[-\frac{(\phi d)^2\pi}{2}\right]\right)}, \tag{8}$$

$$\frac{\partial \ell_+}{\partial \phi} = \frac{d^2}{\phi t W_0\left[-\frac{(\phi d)^2\pi}{2}\right]\left(1 + W_0\left[-\frac{(\phi d)^2\pi}{2}\right]\right)}. \tag{9}$$

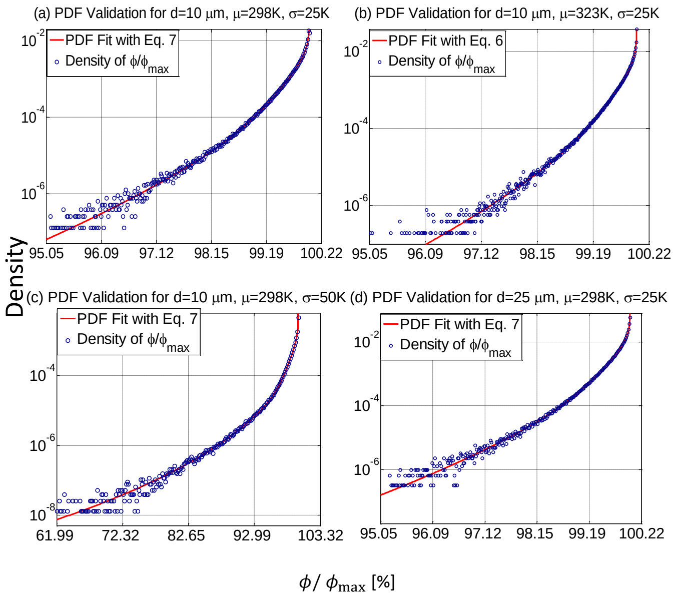

Fig. 2. Plot of density probability of channel fading gain (percentage of peak response) with comparison of simulation results and theoretical derivation

For the purposes of evaluating the channel gain ϕ's distribution (both the CDF and PDF), the value of t is taken at the average optimal sample time $\bar{t}_{\max}$. In the following sections we validate the CDF and PDF that were found by numerical simulations. In our numerical simulations, we assume the temperature changed at the start of each symbol interval and we repeat 10^6 times to produce sufficient results for each figure.

B. Validation of Channel Gain

In Fig. 2, we validate the theoretical PDF given in Eq. (7) using numerical simulation for different transmission distances and temperature variance values. The results in Fig. 2(a) and (b) show that, with the increase of temperature mean value μ by 25K, the fading gain percentage increases less than 1%. By comparison of (a) and (c), the temperature standard deviation σ dominates the fading gain percentage(i.e., a $+25$K increase of σ causes a 30% decrease in the channel gain percentage). Subplots (a) and (d) compares the influence of the distance d. We can observe that d does not have a significant impact on the normalized fading gain percentage $\phi/\phi_{\max}$ as d only affects the value of $t_{\max}$ (Eq. 2) and $\phi_{\max}$.

C. PDF of Channel Gain with Noise

Previously, we have defined the additive noise n as *counting noise* which is Gaussian distributed random variable with zero mean and standard deviation is given as $\sigma_n = \sqrt{\frac{\phi x}{d}}$ [4] in 1-dimension environment. The generic received signal y is a sum of two random variables namely channel gain ϕ and noise n (with a probability density function $f_N(n)$). Therefore, the pdf of y can be given as the integral of both the probability density function of ϕ and n:

$$f_Y(y) = \int_0^{\infty} f_{\Phi,N}(\phi, y-\phi)\mathrm{d}\phi \qquad (10)$$

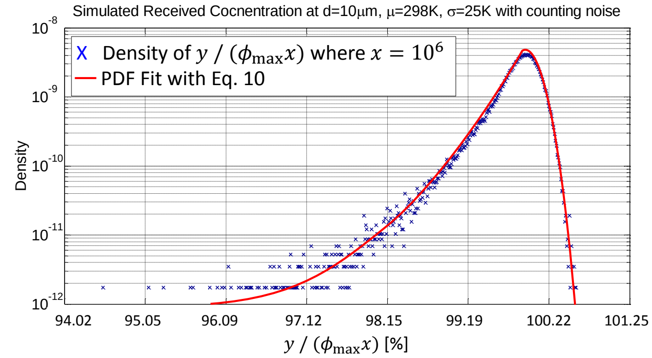

Fig. 3. Plot of simulation for the PDF of generic reveived signal with comparison of theoretical derived PDF $f_Y(y)$

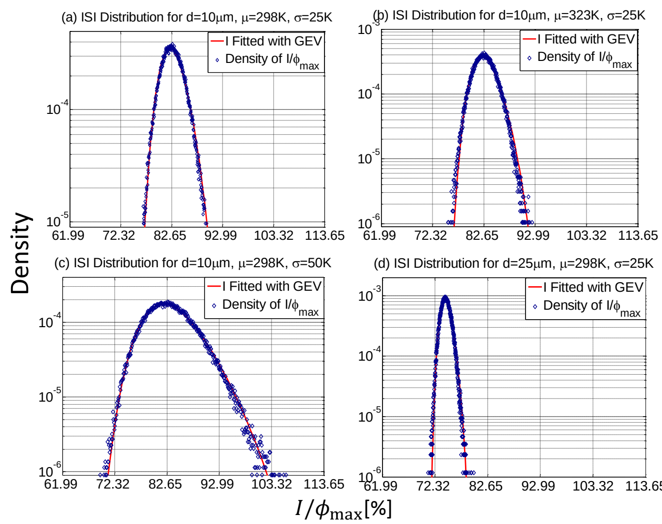

Fig. 4. Plot of simulated ISI distribution and its Generalized Extreme Value (GEV) fitted distribution with parameters: (a) $k_g = -0.17, \mu_g = 39623.5, \sigma_g = 1069.34$, (b) $k_g = -0.15, \mu_g = 39638.1, \sigma_g = 980.92$, (c) $k_g = -0.02, \mu_g = 39369.5, \sigma_g = 2118.72$ and (d) $k_g = -0.15, \mu_g = 15844.8, \sigma_g = 423.92$.

where $f_{\Phi,N}(\phi, y-\phi)$ can be calculated from the derivative of the product of the conditioning probability $P(y-\phi \mid \phi)$ and marginal probability function $P(\phi)$. In Fig. 3, we show the comparison between the simulation results of the generic received signal and the theoretical derived PDF in Eq. (10).

III. Impact on Inter-Symbol-Interference (ISI)

The ISI can arise from multiple previous symbols (heavy-tail of channel response). Similar to previous research [14], [15], we also consider a number of previous symbols that can accurately represent ISI (i.e., 10 symbols). The ISI for a OOK system with a constant symbol period T_s can generally be expressed as the sum of interference from M previous symbols:

$$I(d,t) = \sum_{m=1}^{M} \phi_m(d, \bar{t}_{\max} + mT_s)a_m, \qquad (11)$$

where a_m is the line-coding output and can take on the value 1 or 0. When we come to consider the effect of channel gain on ISI, we can utilize the generic channel gain ϕ's distribution derived in Eq. (6), and assume that the line-code a_m follows some distribution, i.e., P_1 of $a_m = 1$ and $1 - P_1$ of $a_m = 0$.

In Fig. 4, we first assume $P_1 = 0.5$ and we consider the ISI from 10 previous symbols. In the simulation, the channel response for each interference symbol has a fading distribution that is i.i.d. in accordance to Eq. (1) and Eq. (3). We plot the ISI PDF with different transmission distances and temperature variation statistics. We first show that the ISI density distribution can be fitted by a Generalized Extreme Value (GEV) distribution [16] with parameters k_g, μ_g and σ_g. The results indicate that only the standard deviation of the temperature variations strongly affect the ISI distribution. The detailed results in Fig. 4 show that with an increase in mean temperature μ, the distribution in subplots (a) and (b) remains similar. In subplots (a) and (c), as the temperature standard deviation σ increases, the ISI distribution shifts to a higher GEV shape factor k_g, while the range of the ISI stretches significantly. The change of distance does not have obvious effects on the shape of ISI distribution and the percentage of ISI over $\phi_{\max}$ according to subplots (a) and (d) which is similar to our finding in Fig. 2.

IV. Conclusions

In this paper, we have derived the statistical distribution of the channel gain, subject to quasi-static temperature fluctuations. We showed that if the temperature fluctuations follow a Normal distribution, then the channel gain distribution follows a closed form expression. This is important in a communication context, whereby each detected pulse's amplitude will now be subject to variations as a function of the temperature variations in the channel. We further derive the joint distribution of the channel gain and the additive noise, and demonstrate that the temperature variations affect the ISI (a key challenge in the physical layer of molecular communication) where the ISI conforms to a GEV distribution. These distributions can be used by future researchers to obtain more realistic MCvD performances for both micro-scale biological environments and the macro-scale industrial environments.

Appendix

The experiment to measure the temperature variations was setup with a temperature data-logger. A number of temperature data-loggers are deployed around the lab over a continuous period of *24 hours* to record the variations (0.1 degree accuracy) every 30 minutes. The conditions of the lab are uncontrolled in the sense that there is free movement of people and objects. The peak temperature variations varied by up to 2 degrees Celsius which translates to $\approx 8\%$ diffusivity D change (see Eq. 3). The rate of change is slow (a few minutes) and the distance separation between uncorrelated channels is approximately a few metres. Fig. 5 shows an example pdf of temperature distribution at a particular location. The Normal distribution found empirically also conforms to the commonly used Gaussian distribution applied to model in body temperature fluctuations.

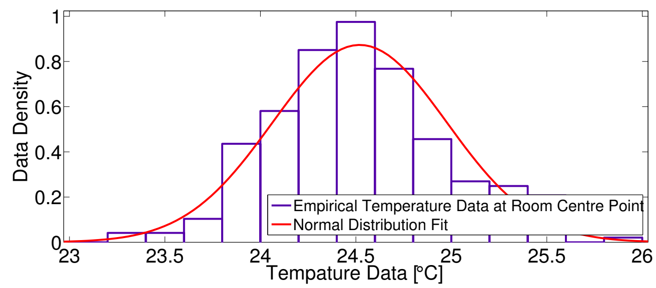

Fig. 5. Probability density plot of temperature distribution at centre of room fitted with Normal Distribution $\mu = 24.52, \sigma = 0.457$.

References

[1] I. Akyildiz, M. Pierobon, S. Balasubramaniam, and Y. Koucheryavy, "The Internet of Bio-Nano Things," *IEEE Communications Magazine*, vol. 53, no. 3, pp. 32–40, Mar. 2015.

[2] W. Guo, T. Asyhari, N. Farsad, H. Yilmaz, B. Li, A. Eckford, and C. Chae, "Molecular Communications: Channel Model and Physical Layer Techniques," *IEEE Wireless Communications*, vol. in press, 2016.

[3] M. Pierobon and I. F. Akyildiz, "Diffusion-Based Noise Analysis for Molecular Communication in Nanonetworks," *IEEE Transactions on Signal Processing*, vol. 59, no. 6, pp. 2532–2547, June 2011.

[4] I. Llaster, A. Cabellos-Aparicio, M. Pierobon, and E. Alarcon, "Detection Techniques for Diffusion-based Molecular Communication," *IEEE Journal on Selected Areas in Communications (JSAC)*, vol. 31, no. 12, pp. 726–734, Jan. 2014.

[5] V. Jamali, A. Ahmadzadeh, C. Jardin, H. Sticht, and R. Schober, "Channel Estimation Techniques for Diffusion-based Molecular Communications," in *2016 IEEE International Conference on Communications (ICC)*, May 2016, pp. 1–7.

[6] C. Bai, M. Leeson, and M. Higgins, "Minimum Energy Channel Codes for Molecular Communications," *Electronics Letters*, vol. 50, no. 23, pp. 1669–1671, Nov. 2014.

[7] U. Chude-Okonkwo, S. Nunoo, and R. Ngah, "Diffusion-based Molecular Communication Concentration and Capacity Dependencies on Human Body Temperature Variation," in *IEEE International Colloquium on Signal Processing and its Applications (CSPA)*, April 2014.

[8] H. Lodish, A. Berk, and S. Z. et al., *Molecular Cell Biology, 4th Edition*. W. H. Freeman and Company, 2000.

[9] W. Guo, S. Wang, A. Eckford, and J. Wu, "Reliable Communication Envelopes of Molecular Diffusion Channels," *Electronics Letters*, vol. 49, no. 19, pp. 1248–1249, Sep. 2013.

[10] S. Qiu, W. Guo, S. Wang, N. Farsad, and A. Eckford, "A Molecular Communication Link for Monitoring in Confined Environments," in *IEEE International Conference on Communications (ICC)- Workshop*, June 2014, pp. 718–723.

[11] H. B. Yilmaz, A. C. Heren, T. Tugcu, and C.-B. Chae, "Three-Dimensional Channel Characteristics for Molecular Communications With an Absorbing Receiver," *IEEE Communications Letters*, vol. 18, no. 6, April 2014.

[12] P. A. Mackowiak, S. S. Wasserman, and M. M. Levine, "A Critical Appraisal of 98.6 F, The Upper Limit of The Normal Body Temperature, and Other Legacies of Carl Reinhold August Wunderlich," *Jama*, vol. 268, no. 12, pp. 1578–1580, Sept. 1992.

[13] T. Nakano, A. Eckford, and T. Haaguchi, *Molecular Communication*. Cambridge University Press, 2013.

[14] G. Genc, Y. E. Kara, H. B. Yilmaz, and T. Tugcu, "ISI-Aware Modeling and Achievable Rate Analysis of the Diffusion Channel," *IEEE Communications Letters*, vol. 20, no. 9, pp. 1729–1732, June 2016.

[15] B. Tepekule, A. E. Pusane, H. B. Yilmaz, C. B. Chae, and T. Tugcu, "ISI Mitigation Techniques in Molecular Communication," *IEEE Transactions on Molecular, Biological and Multi-Scale Communications*, vol. 1, no. 2, pp. 202–216, June 2015.

[16] L. Wright, *Sea Level Rise, Coastal Engineering, Shorelines and Tides*. Nova Science Publishers, 2011.